Acta Radiologica Open
4(2) 1–7

DOI: 10.1177/2047981614552217
arr.sagepub.com

Adult onset asynchronous multifocal eosinophilic granuloma of bone: an 11-year follow-up

Benjamin Dallaudière[1], Joseph Kerger[2], Jacques Malghem[1], Christine Galant[3] and Frederic E Lecouvet[1]

Abstract

Multifocal eosinophilic granuloma (EG) is a rare observation within the spectrum of histiocytosis X, generally described in children. We report the case of a 33-year-old man with multifocal EG showing an asynchronous evolution of bone lesions during a follow-up of 11 years. We also present the therapeutic approach chosen for this patient and the repeated magnetic resonance imaging (MRI) examinations used to monitor the disease with a final favorable outcome.

Keywords

Granuloma, eosinophilic, Langherans, histiocytosis, bone, tumors, MRI

Date received: 23 January 2014; accepted: 30 August 2014

Introduction

Langerhans cell histiocytosis (LCH) or histiocytosis X has a variable course from a self-limited eosinophilic granuloma (EG) to an aggressive disseminated disease (1). It mainly affects children and is characterized by idiopathic proliferation of histiocytes producing focal or systemic manifestations; its pathogenesis remain unclear (2). In the past, three classic syndromes were described: (i) EG in which the disease is limited to bone in patients usually aged 5–15 years; (ii) Hand-Schüller-Christian disease (HSC), characterized by multifocal bone lesions and extraskeletal involvement of the reticuloendothelial system usually seen in children aged 1–5 years; and (iii) Letterer-Siwe disease (LS), characterized by disseminated involvement of the reticuloendothelial system in children aged less than 2 years (2,3). Subsequently, according to modern literature, all these syndromes are encompassed in Langerhans cell histocytosis (LCH). Indeed, the Langerhans cell of the skin was proposed as the underlying shared pathologic feature among these three disorders despite different gene expression according to their localization (4).

To our knowledge, the skull, ribs, mandible, clavicle, pelvis, and long bones are the most frequently involved sites in EG (5). Spinal disease is rare (7–15%) in adults (6). Indeed, fewer than 30 cases of spinal EG have been described in adults in the literature (7,8).

We report a 33-year-old man with multifocal bone EG, involving the spine, ribs, sacrum, iliac bones, and femurs. The diagnosis was established by histological examination. The disease course was monitored using magnetic resonance imaging (MRI) of the axial skeleton during an 11-year follow-up, illustrating the asynchronous evolution of the lesions with spontaneous healing of some lesions, appearance and disappearance of new lesions with eventual disappearance of lesions. This favorable outcome was observed after ''minimally invasive'' treatment mainly consisting of antalgic and

[1]Department of Radiology, Centre du Cancer et Institut de Recherche Expérimentale et Clinique (IREC), Cliniques Universitaires Saint Luc, Université Catholique de Louvain, Brussels, Belgium
[2]Department of Oncology, Institut Jules Bordet, Brussels, Belgium
[3]Department of Pathology, Cliniques Universitaires Saint Luc, Brussels, Belgium

Corresponding author:
Frederic E Lecouvet, Department of Radiology, Cliniques Universitaires Saint Luc, Université Catholique de Louvain, Bruxelles. Avenue Hippocrate, Brussels, Belgium.
Email: frederic.lecouvet@uclouvain.be

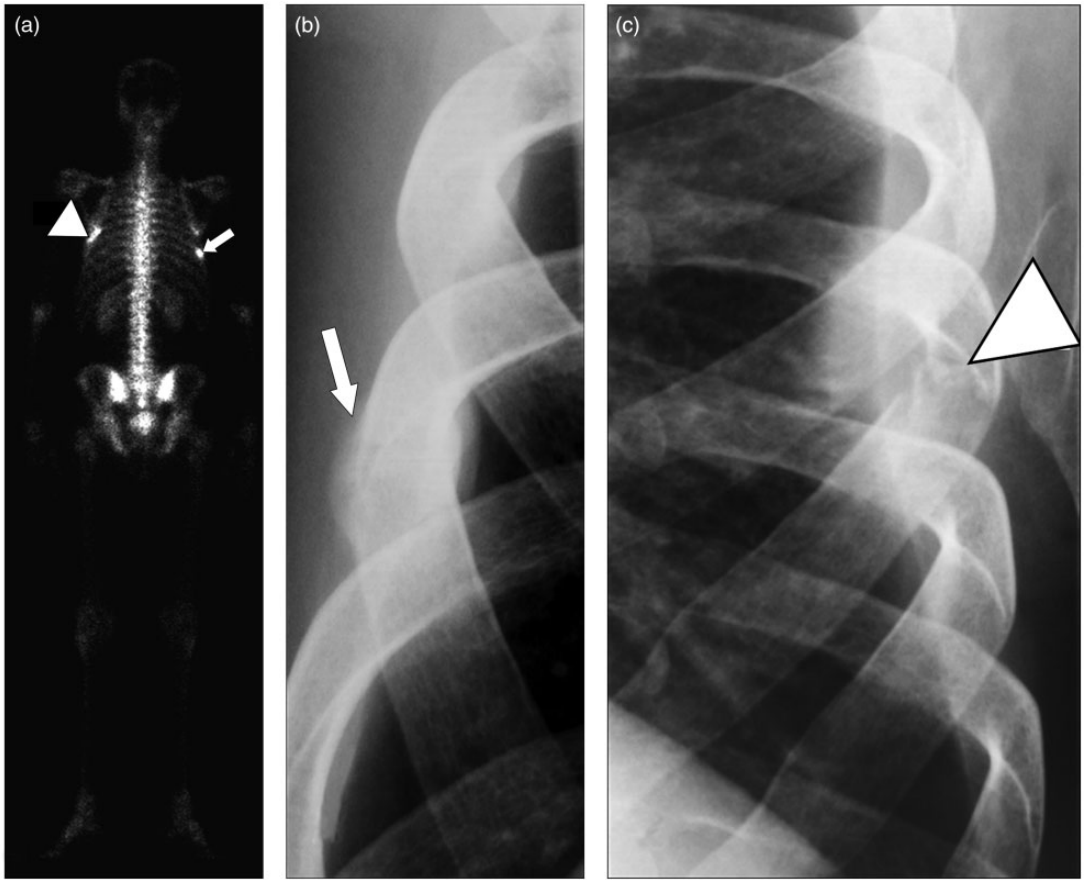

Fig. 1. Posterior-anterior bone scintigraphy shows (a) increased uptake in the mid portion of the eighth right rib (white arrow) and in the posterior aspect of the eighth left rib (white arrowhead). On radiographs, these foci corresponded to (b) an older fracture of the eighth right rib with osteosclerosis and periosteal reaction (white arrow) and (c) a recent pathological fracture of the eighth left rib without periosteal reaction (white arrowhead).

bisphosphonate cycles after early cervical laminectomy and T3 vertebroplasty.

Case report

A 33-year-old Caucasian male patient was referred in March 2002 for a 2-month history of severe bilateral rib pain, predominating on the left side and irradiating to the cervical spine, resistant to painkillers.

Clinical examination only revealed cervical contracture. Laboratory investigations revealed mild inflammatory syndrome: C-reactive protein (CRP) level was minimally increased at 1.2 mg/dl and fibrinogen at 535 g/L.

Initial imaging work-up included Technetium$^{99\,m}$ bone scintigraphy (BS) and radiographs of the thoracic girdle. The BS showed increased uptake in the mid-portion of the eighth right rib and in the posterior aspect of the eighth left rib with no abnormalities in the cervical spine. Radiographs confirmed these lesions and revealed a recent pathological fracture of the eighth left rib and also an older fracture of the eighth right rib with osteosclerosis and periosteal reactions (Fig. 1a–c). A computed tomography (CT) scan showed a healing process in the eighth right rib, large osteolysis in the eighth left rib, but also an incidental asymptomatic osteolysis in the posterior arch of seventh cervical vertebra (C7), in the manubrium sterni and in the left iliac bone (Fig. 2a–c). MRI was performed to characterize these lesions, which consisted of bone marrow replacement with decreased signal intensity on T1-weighted (T1W) images and increased signal intensity on T2-weighted (T2W) images. MRI also revealed asymptomatic foci of marrow replacement in the T3, T11, and L5 vertebral bodies and in the right femoral neck (Figs. 3 and 4).

A CT-guided percutaneous needle biopsy of the eighth left rib fracture was obtained showing bone infiltration by eosinophilic leucocytes and numerous histiocytes, with some of them being multinucleated.

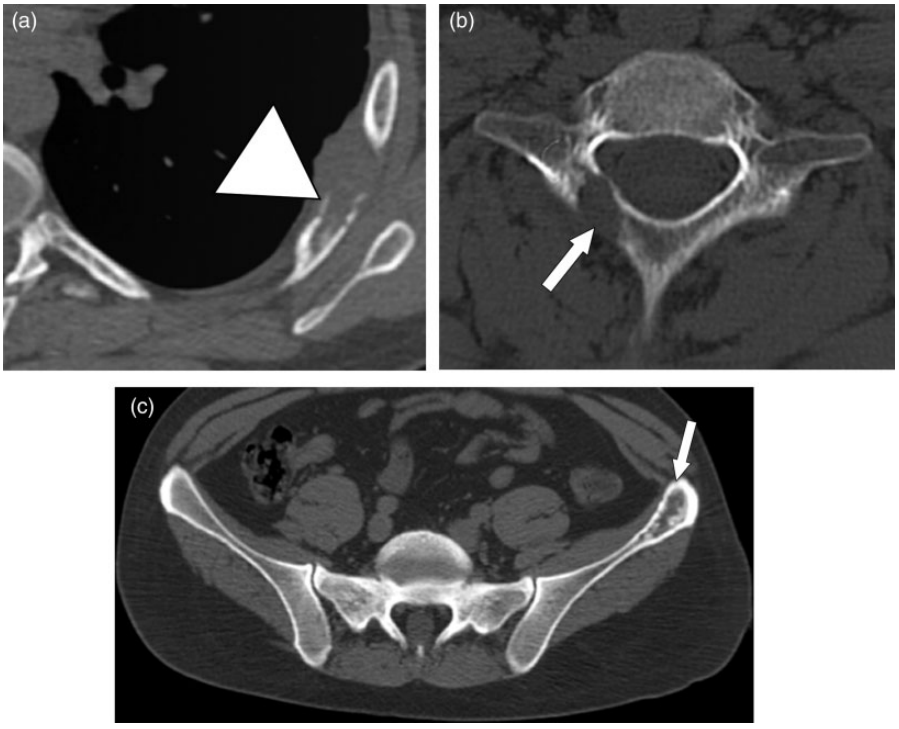

Fig. 2. CT scan shows (a) focal osteolysis in the eighth left rib with adjacent soft tissue swelling (white arrowhead), (b) in the posterior arch of C7 (white arrow), and (c) mixed lytic and sclerotic lesion in the left anterior part of iliac bone (white arrow).

Fig. 3. Coronal T1W MRI sequence shows bone marrow replacement (decreased signal intensity on T1) in the left iliac bone (white arrowhead) and in the right femoral neck (white arrow).

(Fig. 5a, b). Immunohistochemically, they expressed reactivity for S100-protein and CD 1A. A blind bone marrow biopsy of the right iliac bone was obtained to rule out diffuse malignant infiltration and showed no abnormality.

Medical antalgic treatment with cervical physiotherapy was initiated, leading to initial symptomatic improvement.

Two months later in May 2002, the patient was readmitted for severe thoracic spine pain. CT and MRI showed a pathological compression fracture of the T3 vertebra (Fig. 6). CT additionally showed favorable evolution of the eighth left rib (Fig. 7) and of the T11 lytic lesions with ongoing centripetal reconstruction. All the other lesions were stable except for an increase in size of the L5 vertebral body lesion, and appearance of a new lesion within the left femoral neck. All these lesions were asymptomatic. The T3 fracture was treated by cementoplasty with good functional results and medical treatment was continued.

Three months later in August 2002, because of severe cervical pain, a C7 laminectomy was performed. All lesions were stable except at imaging for the appearance of a new asymptomatic lesion in the L2 body. Follow-up MRI showed bilateral healing of the femoral neck lesions with appearance of fatty signal within the lesions, and disappearance of the L5 lesion. At this stage, initiation of systemic treatment was proposed to the patient: as he was reluctant to start cytotoxic vinblastin- or etoposide-based chemotherapy together with corticosteroids, and because of the essentially osteolytic nature of the EG lesions, we finally started an empirical intravenous bisphosphonate therapy consisting initially in monthly intravenous administrations of 4 mg of zoledronic acid for 2 years, thereafter 2-monthly infusions for another period of 2 years and finally 3-monthly injections.

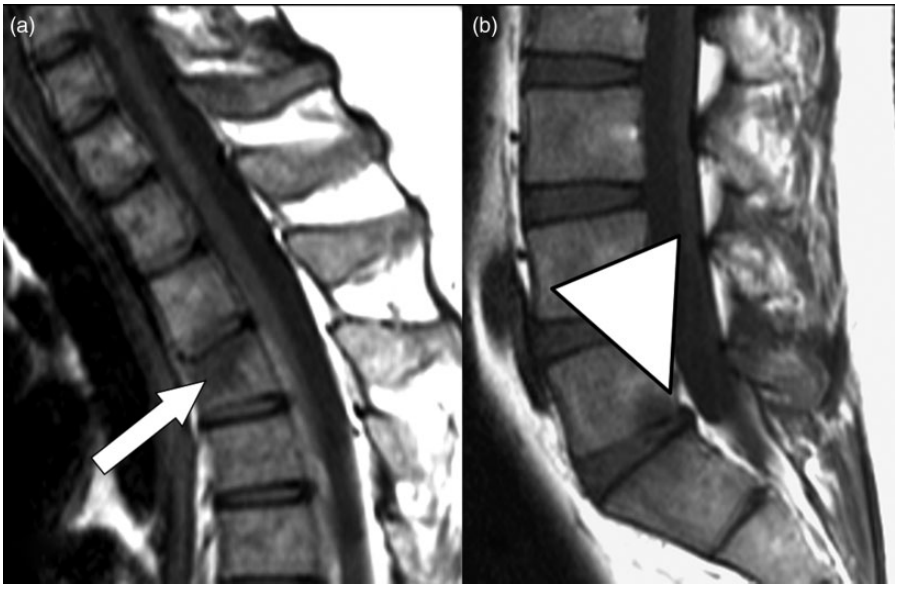

Fig. 4. (a, b) Sagittal T1W MRI sequence shows bone marrow replacement and in T3, with small vertebral deformity (arrow in a) and in the L5 vertebral body (arrow head in b).

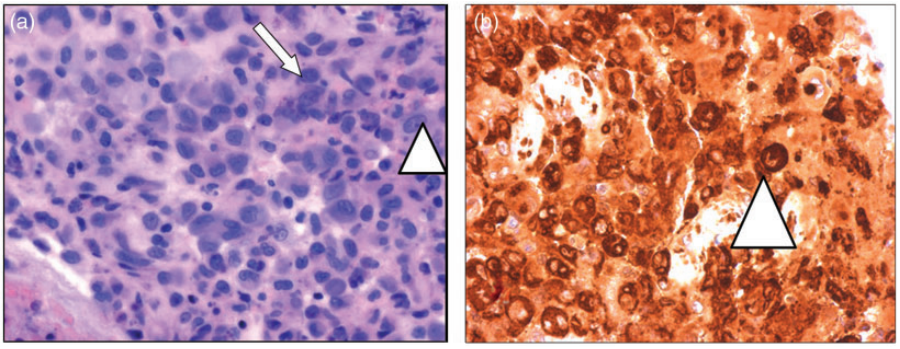

Fig. 5. (a, b) Histopathology of the bone biopsy from the eighth left rib shows infiltration by eosinophilic leucocytes (arrow in a) and numerous histiocytes, with some of them being multinucleated (arrowhead in a) with expression reactivity for S100-protein and CD 1A on immunohistochemistry (arrowhead in b).

A 10-month MRI follow-up, in June 2003, showed regression of the left iliac and L2 lesions, with appearance of a new left sacral lesion. The 12-month MRI follow-up (August 2003) showed an asynchronous evolution of the lesions with fading of all lesions replaced by an increase of the focal fat content, except for the left sacral lesion. The patient remained asymptomatic.

At a December 2004 follow-up, the left sacral lesion showed involution to fatty marrow. The patient was then systematically followed-up with MRI every 6 months from December 2004 until April 2013. In 2009, a "last" new L5 vertebral body lesion appeared under the same systemic treatment with analgesics and 3-month intervals intravenous infusions of zoledronic acid and remained asymptomatic. Finally, all lesions except this L5 body lesion had disappeared by the end of 2013, under the same antalgic and biphosphonates regimens (Figs. 8 and 9), and only a small residual area of abnormal marrow signal remains visible in L5 (presumed scar tissue), stable in size from 2009 to 2013 (Fig. 10).

Discussion

In this patient, the diagnosis of EG was suspected because of the clinical history, patient age, and imaging appearance of the lesions. In this case, CT findings were non-specific, mainly consisting in large osteolytic defects, with sclerosis in some of them suggestive of

Fig. 6. Two months later, sagittal T1W MR image shows a progressive pathological compression fracture of the T3 vertebra (arrow, compared with Fig. 4a).

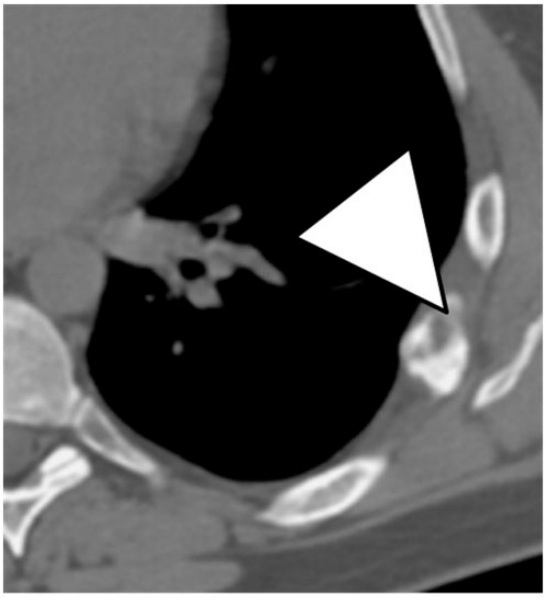

Fig. 7. Two months later, CT scan shows favorable evolution of the eighth left rib lesion with ongoing centripetal reconstruction (arrowhead, compared with Fig. 2a).

spontaneous lesion healing. The MRI appearance was a non-specific bone marrow replacement (3).

The radiographic appearance of osseous EG varies according to the involved site and phase of the disease. Early lesions appear aggressive, osteolytic, with poorly defined margins, sometimes with lamellar periosteal reactions. Later on, lesions appear well defined and may show sclerotic margins and expansile contours (2).

At MRI, non-specific bone marrow replacement is visible as low signal on T1W and high signal on T2W images, including differential diagnoses such as neoplastic lesions like myeloma, metastasis, lymphoma foci, or benign tumors (9–11). In our patient, lesion healing was observed on follow-up imaging, characterized by fat signal reappearance within the lesions.

The final diagnosis was established by percutaneous biopsy under CT guidance. Histology was typical with eosinophilic leucocytes and numerous histiocytes. In the literature, asynchronous evolution and multifocal recurrence of EG has been reported by some authors early after disease discovery (12).

The treatment of adult onset EG is not well established, given the rare observation of this condition and several medical or surgical therapeutic approaches have been proposed according to patient age and disease locations (13). In the literature, this wide variety of proposed treatments includes intralesional methylprednisolone injection with clinical benefit and imaging resolution of the lesions (14), systemic and local corticosteroid therapy (15), chemotherapy (1), radiation therapy (16), surgery (17), and surgery in association with chemotherapy with vinblastine (18). Surgery is not recommended in case of spinal lesions because of the significant recurrence risk (17).

In case of failure of these treatments, some authors recommended repeated intraosseous injections of triamcinolone-1 16 alpha 21-diacetate, a synthetic steroid, which could lead to a rapid, complete, and durable resolution (15).

The treatment must be adapted to the characteristics of the patient and lesion locations. No study exists that compares the effectiveness of the different possible treatment approaches.

In the present case and after the literature review of the different therapeutic options we finally chose a systemic treatment consisting in analgesic medications and bisphosphonate treatments, because of the primarily osteolytic pattern, and because the patient was reluctant to undergo cytotoxic chemotherapy (19). Additional local treatment consisting in cementoplasy of a vertebral body, and partial resection of a posterior vertebral arch were also performed, being preferred to curettage because of the risk of local recurrence.

Long-term follow-up with repeated MRI studies proved the effectiveness of this approach. The

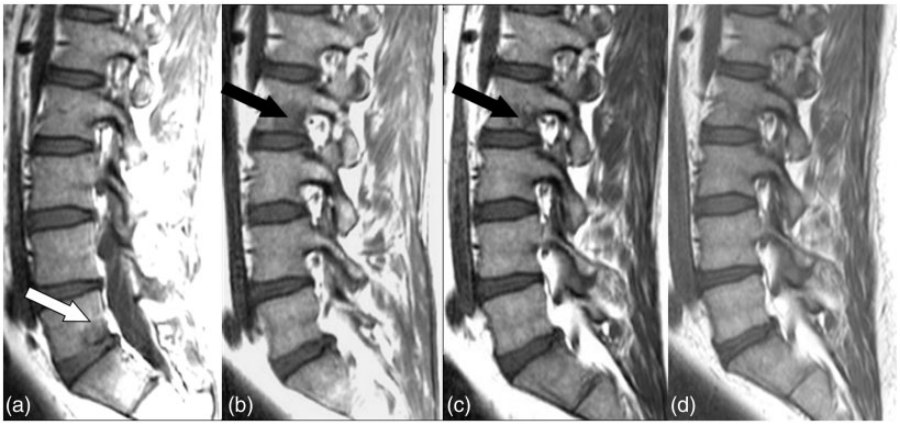

Fig. 8. (a–d) Consecutive sagittal T1W MRI studies show the asynchronous evolution (appearance, then involution) of L2 (black arrow) and L5 (involution) (white arrow) vertebral body lesions with decrease in size and reappearance of fat at the periphery of the lesions and final healing.

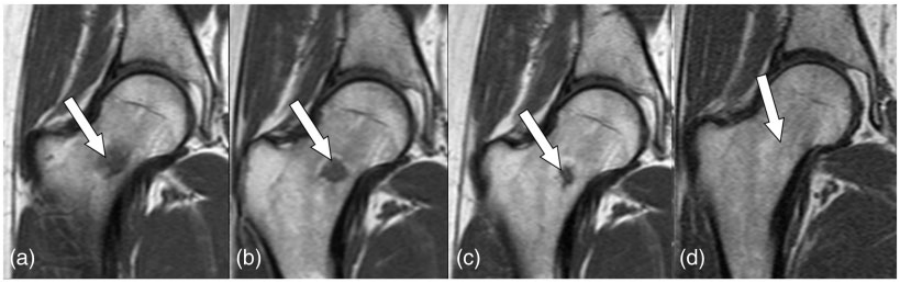

Fig. 9. (a–d) Consecutive coronal T1W studies of the pelvis show decrease in size of the right femoral neck lesion with reappearance of fat at the periphery and final healing (arrow).

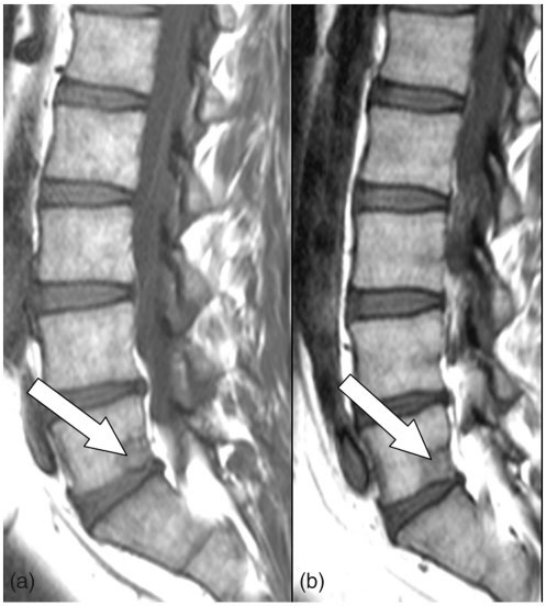

Fig. 10. (a, b) Systematic spine MRI follow-up shows on sagittal T1W images small low signal lesion of L5 vertebral body (arrow in a) lesion, appearing in 2009, with no change during the following 4 years (arrow in b), presumed to represent inactive lesion or scar tissue.

singularity of this case relies on the multiplicity of lesions, some being asymptomatic, others being responsible for pathologic fractures, and most importantly on the asynchronous evolution of these lesions, showing spontaneous involution of some of them, appearance of new foci, with subsequent involution.

Most lesions involved the axial skeleton (i.e. spine, ribs, pelvis and proximal femur). Finally, the disease course was mainly evolutive during 2 years, and the subsequent 9-year follow-up MRI studies showed return to almost normal marrow appearance, during which time 3-month intervals intravenous bisphosphonate injections were pursued (up to 2013).

In conclusion, we report an exceptional long-term clinical and MRI follow-up of multiple EG observed in an adult, showing the asynchronicity of the lesions with a final favorable outcome after empirical therapeutic approach and a total follow-up period of more than 11 years.

Acknowledgements

The authors wish to thank Dr Z El Ali, Dr P Omoumi, and Dr A Larbi for their fruitful collaboration.

Conflict of interest

The authors have no conflict of interest to disclose.

References

1. Lahiani D. Hammami BK, Maâloul I, et al, Multifocal Langerhans cell histiocytosis of bone: late revelation in a 76-year-old woman. Rev Med Interne 2008;29: 249–251.
2. Stull MA, Kransdorf MJ, Devaney KO. Langerhans cell histiocytosis of bone. Radiographics 1992;12:801–823.
3. Boutsen Y, Esselinckx W, Delos M, et al. Adult onset of multifocal eosinophilic granuloma of bone: a longterm follow-up with evaluation of various treatment options and spontaneous healing. Clin Rheumatol 1999; 18:69–73.
4. Allen CE, Li L, Peters TL, et al. Cell-specific gene expression in Langerhans cell histiocytosis lesions reveals a distinct profile compared with epidermal Langerhans cells. J Immunol 2010;184:4557–4567.
5. Huvos AG. *Bone tumors: diagnosis, treatment and prognosis*. Philadelphia, PA: WB Saunders, 1991, pp.695–711.
6. Ueda Y, Murakami H, Demura S, et al. Eosinophilic granuloma of the lumbar spine in an adult. Orthopedics 2012;35:1818–1821.
7. Lauffenburger MD, Dull ST, Toselli R. Eosinophilic granuloma of the adult spine: a case report and review of the literature. J Spinal Disorders 1995;8: 243–248.
8. Montalti M, Amendola L. Solitary eosinophilic granuloma of the adult lumbar spine. Eur Spine J 2012;21: 441–444.
9. Moore JB, Kulkarni R, Crutcher DC, et al. MRI in multifocal eosinophilic granuloma: staging disease and monitoring response to therapy. Am J Pediatr Hematol Oncol 1989;11:174–177.
10. Lang N, Su MY, Yu HJ, et al. Differentiation of myeloma and metastatic cancer in the spine using dynamic contrast-enhanced MRI. Magn Reson Imaging 2013;31: 1285–1291.
11. Thakur NA, Daniels AH, Schiller J, et al. Benign tumors of the spine. J Am Acad Orthop Surg 2012;20:715–724.
12. Sessa S, Sommelet D, Lascombes P, et al. Treatment of Langerhans-cell histiocytosis in children. Experience at the Children's Hospital of Nancy. J Bone Joint Surg Am 1994;76:1513–1525.
13. De Angulo G, Nair S, Lee V, et al. Nonoperative management of solitary eosinophilic granulomas of the calvaria. J Neurosurg Pediatr 2013;12:1–5.
14. Mavrogenis AF, Abati CN, Bosco G, et al. Intralesional methylprednisolone for painful solitary eosinophilic granuloma of the appendicular skeleton in children. J Pediatr Orthop 2012;32:416–422.
15. Watzke IM, Millesi W, Kermer C, et al. Multifocal eosinophilic granuloma of the jaw: long-term follow-up of a novel intraosseous corticoid treatment for recalcitrant lesions. Oral Surg Oral Med Oral Pathol Oral Radiol Endod 2000;90:317–322.
16. Gmelin E, von Lieven H. Radiation therapy of the eosinophilic granuloma of bone. Strahlentherapie 1980; 156:611–615.
17. Vanhoenacker FM, De Beuckeleer LH, De Roeck F, et al. Metachronous eosinophilic granuloma of bone. JBR-BTR 2000;83:234–237.
18. Karagoz Guzey F, Bas NS, Emel E, et al. Polyostotic monosystemic calvarial and spinal Langerhans cell histiocytosis treated by surgery and chemotherapy. Pediatr Neurosurg 2003;38:206–211.
19. Elomaa I, Blomqvist C, Porkka L, et al. Experiences of clodronate treatment of multifocal eosinophilic granuloma of bone. J Intern Med 989;225:59–61.